

Supporting Information

Nitrate respiration and diel migration patterns of diatoms are linked in sediments underneath a microbial mat.

Elisa Merz^{1*}, Gregory J. Dick², Dirk de Beer¹, Sharon Grim², Thomas Hübener³, Sten Littmann¹, Kirk Olsen², Dack Stuart⁴, Gaute Lavik¹, Hannah K. Marchant¹ & Judith M. Klatt^{1,2*}

¹Max Planck Institute for Marine Microbiology, Bremen, Germany

²University of Michigan, Department of Earth & Environmental Sciences, Ann Arbor, MI, USA

³University of Rostock, Institute of Biosciences Department of Botany and Botanical Garden, Germany

⁴University of Michigan, Cooperative Institute for Great Lakes Research, Ann Arbor, MI, USA

*Correspondence to: Elisa Merz (emerz@mpi-bremen.de), Judith Klatt (jklatt@mpi-bremen.de)

Supplementary Methods	2
16S sequencing and analysis	2
Supplementary Figures	4
Supplementary Tables	8
Supplementary References	11

Supplementary Methods

16S sequencing and analysis

From samples collected in 2012 through 2017, up to 0.5 g of wet mat material was extracted using a modified version of the MPBio Fast DNA Spin Kit for Soil (MP Biomedical, Santa Anna, CA, USA). In summary, 0.3 g of beads (corresponding to 1 large bead, 7 medium beads, and an equal volume of small beads), sodium phosphate buffer, and MT buffer was used to chemically and mechanically lyse cells, in either the FastPrep instrument for 45 s (samples up to 2013), or horizontal lysis on a vortex mixer for 10 min at speed 7 (2014 - 2015). After protein precipitation, DNA was cleaned, pelleted, and resuspended in up to 100 μ L nuclease-free water. DNA was stored at 4°C for immediate quantification and -20°C for long term.

A PicoGreen assay (Invitrogen, Carlsbad, CA, USA) was used to quantitate double stranded DNA. Samples were diluted to between 1-25 ng/ μ L and submitted to the University of Michigan Host Microbiome Core for Illumina library preparation and sequencing (Seekatz et al. 2015; Kozich et al. 2013). Bacterial primers 515F/806R were used to amplify the 16S rRNA gene v4 region in a reaction mixture consisting of 5 μ L of 4 μ M equimolar primer set, 0.15 μ L of AccuPrime Taq DNA High Fidelity Polymerase, 2 μ L of 10x AccuPrime PCR Buffer II (Thermo Fisher Scientific), 11.85 μ L of PCR-grade water, and 1-10 μ L of DNA template. Thermocycling was an initial denaturation at 95°C for 2 min, 30 cycles of 95°C for 20 s, 55°C for 15 s, 72°C for 5 min, and a final extension of 72°C for 10 min. PCR products were cleaned and normalised using SequalPrep Normalisation Plate Kit (Thermo Fisher Scientific), then quantified and pooled equimolarly according to Kapa Biosystems Library qPCR MasterMix (ROX Low) Quantification kit for Illumina platforms. An Agilent Bioanalyzer kit confirmed library size and purity, and the library pool was sequenced on the Illumina MiSeq using a 500 cycle V2 kit with 15% PhiX for diversity.

Raw pairs of sequencing reads (250 bp) were quality trimmed and merged using ‘iu-merge-pairs’, which is a program in illumina-utils (available from <https://github.com/merenlab/illumina-utils>) (Eren et al. 2013), using minimum quality score of 25, minimum overlap of 200 bp, and at points of divergence in the overlap the higher quality basecall was retained. Merged reads with 5 or fewer mismatches were kept for Minimum Entropy Decomposition v. 2.1 (Eren et al. 2015) using the following parameters: -d 4 -N 3 --min-substantive-abundance 5 -V 3 --relocate-outliers. GAST (Huse et al. 2008) was used to call taxonomy using the curated SILVA database, and confirmed with BLASTN against SILVA 123 (Pruesse et al. 2007) (bacteria and archaea), and PhytoRef (Decelle et al. 2015) (chloroplasts). mothur v. 1.33 (Schloss et al. 2009) was used to check for chimeras de novo, and putatively-chimeric nodes that did not have taxonomy assigned via SILVA 123 and GAST were removed. The R statistical environment (R Core Team 2015) in RStudio (RStudio Team 2014) was used to analyse nodes.

Sequence data have been submitted to the GenBank database under accession number PRJNA305364 (<https://www.ncbi.nlm.nih.gov/bioproject/PRJNA305364>).

Supplementary Figures

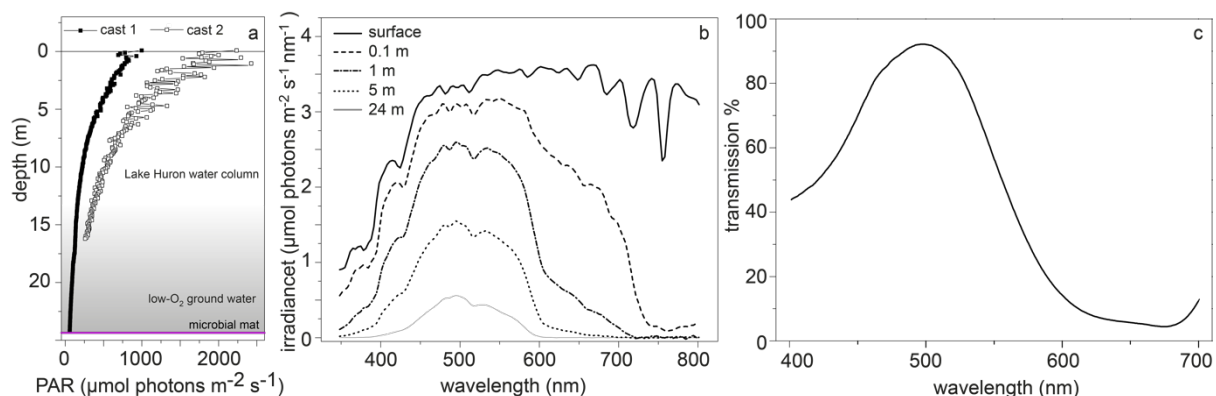


Figure S1: a) Depth profiles of photosynthetically active radiation (PAR) derived from downwelling irradiance spectra obtained during two casts of a Sea-Bird HyperPro II profiler equipped with up- and down-facing HyperOCR radiometers. Grey area indicates the low-O₂ groundwater layer below the Lake Huron water column, with hydrology-dependent variable height (0.5 – 8 m) above the mat surface (purple line) b) Irradiance spectra from cast 1 at the: surface (black line), 0.1 m (dashed line), 1 m (dot-dash-line), 5 m (dotted line), and 24 m (greyline) below the water surface. c) Transmission spectrum of visible light through the optical filter foil used for illumination of cores and batch incubations for stable isotope incubation experiments.

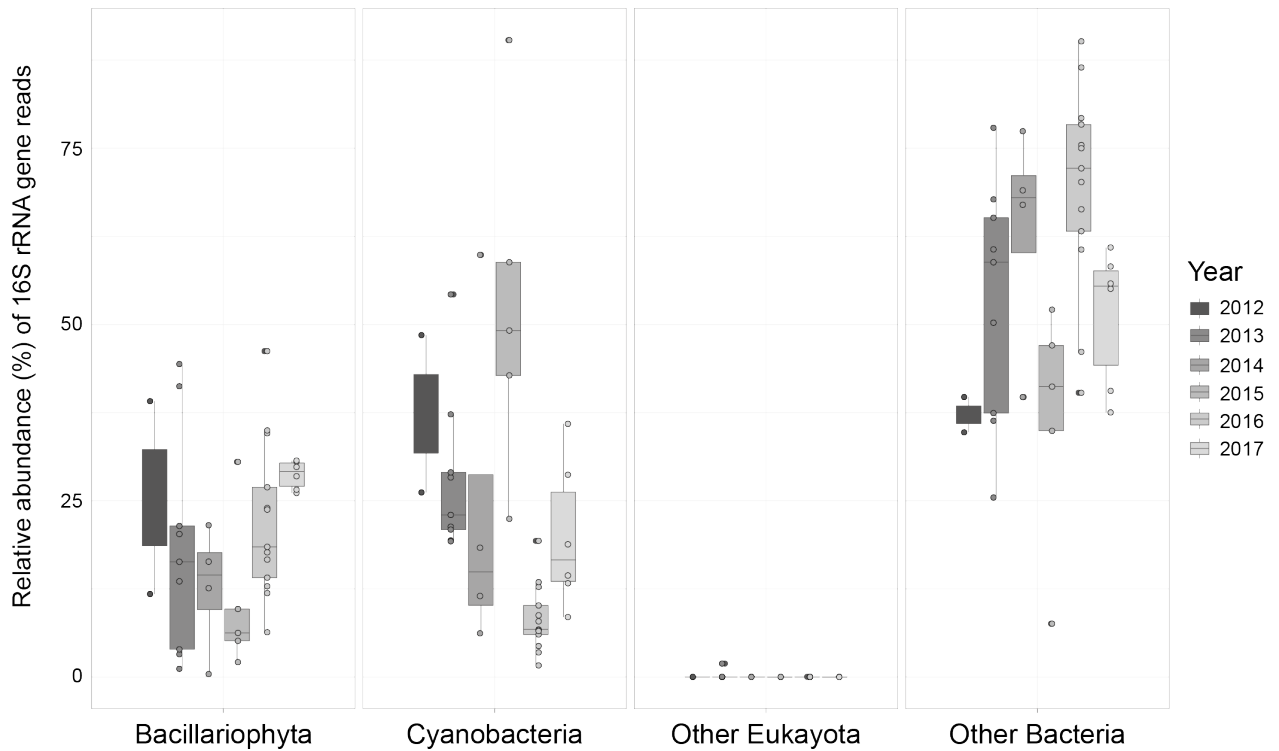


Figure S2: Distribution of 16S rRNA gene relative abundance of interesting taxonomic groups: Cyanobacteria and Bacillariophyta (diatoms). Chloroplast genes belonging to the Bacillariophyta were the most widely observed of identifiable 16S rRNA genes. They contributed up to 46% of the reads in each sample, comparable to the contribution of cyanobacterial reads. Only up to 2% of reads in each sample belonged to other eukaryotes. Over multiple years and months, the microbial mat was sampled for the 16S rRNA gene via Illumina tag sequencing. Data from the most recent year (2017) surveyed are presented in light grey, whereas data from the oldest year surveyed (2012) are plotted in dark grey.

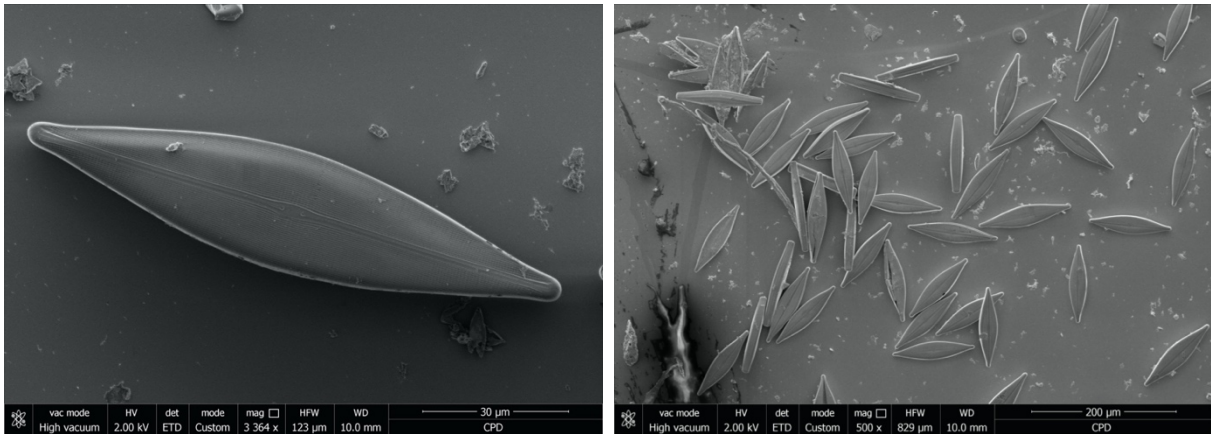


Figure S3: SEM images of *Craticula cuspidata* from the Middle Island Sinkhole. Morphological features allowing to differentiate between the two sister taxa *Craticula cuspidata* and *Craticula acidoclinata* Lange-Bertalot & Metzeltin, 1996 are not apparent in light microscopy images because both freshwater elliptic-lanceolate taxa are similar in size and general morphology. Namely Middle Island Sinkhole diatoms measure 98-123 x 24-28 μm (length x width) which is in the range of both *C. cuspidata* (65-170 x 17-35 μm) and *C. acidoclinata* (60-130 x 16-24 μm) (Lange-Bertalot, 2001). SEM revealed the Middle Island Sinkhole diatom has 11-12 and 10-15 striae/10 μm centre and apical ends, respectively, leaning with their description towards *C. cuspidata* rather than *C. acidoclinata*. Furthermore, the small axial area is much narrower in *C. cuspidata* compared to *C. acidoclinata* and the central area in *C. cuspidata* is nearly absent, but moderately large in *C. acidoclinata*. Thus, the Middle Island Sinkhole diatoms were identified as *C. cuspidata*. This conclusion is consistent also with differences in the preferred autecological conditions of the two *Craticula* species. *C. cuspidata* is found in aquatic ecosystems with higher electrolyte content and even survives in brackish waters, whereas *C. acidoclinata* mainly occurs in low-electrolyte, oligotrophic mostly dystrophic waters distinct from the conditions in the Middle Island Sinkhole.

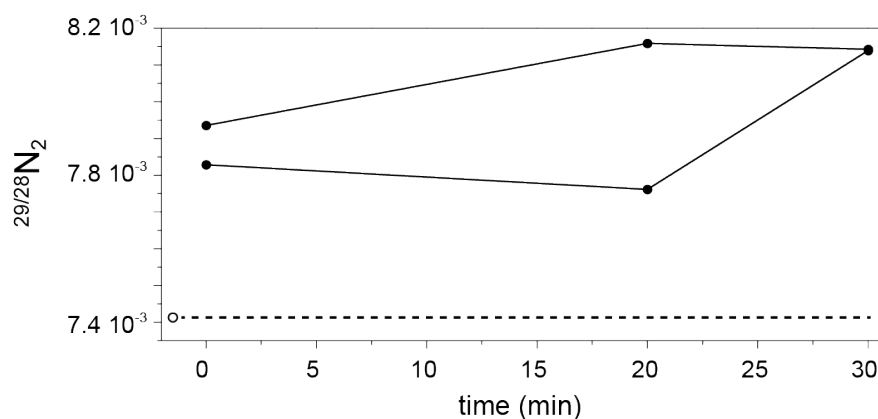


Figure S4: $^{15}\text{NO}_3^-$ uptake by diatoms pre-fed with $^{14}\text{NO}_3^-$. To determine the rate of uptake of externally supplied $^{15}\text{NO}_3^-$, diatoms that had been pre-fed for 24 h with $^{14}\text{NO}_3^-$ were transferred to $^{15}\text{NO}_3^-$ amended in-situ water and incubated in the dark. The incubation was stopped after 0, 10, 20 and 30 min by filtering the tube contents. The filter was washed with 10 ml deionised water and exposed to thaw-freeze cycles to release internally stored $^{15}\text{NO}_3^-$. $^{15}\text{NO}_3^-$ in the cracked diatom samples was measured as $^{29}\text{N}_2/^{28}\text{N}_2$ after cadmium and sulfamic acid reduction to N_2 (after initial $^{15}\text{NO}_2^-$ removal using sulfamic acid). The open circle and dashed line is the $^{29}\text{N}_2/^{28}\text{N}_2$ ratio in the diatoms after the 24 h pre-feeding period with $^{14}\text{NO}_3^-$ and before the $^{15}\text{NO}_3^-$ addition. After $^{15}\text{NO}_3^-$ addition, the $^{29}\text{N}_2/^{28}\text{N}_2$ ratio in the diatoms increased instantaneously (closed, connected circles; in duplicates) compared to this background value and remained approximately constant.

Supplementary Tables

Table S1: Initial areal rates of $^{15}\text{NO}_3^-$ respiration by DNRA and denitrification in batch incubations (Fig. 1). Rates were calculated based on the slope of $^{15}\text{NH}_4^+$ and $^{30}\text{N}_2$, $^{29}\text{N}_2$ concentration increase within the first three hours after tracer addition for: mat and mat-sediment, and 6 h after tracer addition for the sediment incubation due to insufficiently dense sampling intervals. Values in parentheses represent R^2 values from linear regression fitting, forced through zero.

	Mat	Sediment	Mat + Sediment
DNRA ($\mu\text{mol } ^{15}\text{NO}_3^- \text{ m}^{-2} \text{ s}^{-1}$)	420.0 (0.31)	1078.2 (0.91)	2936.5 (0.28)
Denitrification ($\mu\text{mol } ^{15}\text{NO}_3^- \text{ m}^{-2} \text{ s}^{-1}$)	2.8 (0.017)	26.5 (0.78)	16.1 (0.39)

Table S2: Volumetric rates of $^{15}\text{NH}_4^+$ production ($\mu\text{M h}^{-1}$) in depth sections over a simulated diel cycle used for Figure 4a. For plotting, the missing time and depth points (— = no data) were added by interpolation. Shaded rows indicate exposure of the cores to darkness.

	$^{15}\text{NH}_4^+$ production rate ($\mu\text{M h}^{-1}$) in depth section				
	0 – 0.5 cm	0.5 – 1 cm	1 – 2 cm	2 – 3 cm	3 – 4 cm
16:00	-3.44	51.53	2.90	-2.40	-1.80
18:00	12.93	45.46	39.99	1.90	6.98
21:00	109.60	-8.52	76.97	47.84	3.14
00:30	88.63	26.37	0.17	74.00	75.31
01:00	6.66	3.10	-1.43	32.42	61.18
02:00	4.40	—	7.58	8.36	3.33
02:45	23.25	11.10	-1.90	1.45	21.33
04:30	12.94	-1.95	0.95	-1.71	81.53
04:45	29.57	10.25	-2.55	2.29	87.78
05:21	-2.15	20.47	4.59	61.79	59.09
06:21	2.95	2.22	10.57	84.20	7.79
07:30	-2.55	-6.13	2.85	52.98	1.38
07:00	-0.14	5.43	25.35	42.36	5.41
08:30	32.86	14.26	87.69	15.60	-8.17
09:30	-6.43	4.31	97.88	8.33	2.96
09:15	-7.53	13.33	55.76	17.22	—
10:45	-0.49	195.81	63.90	—	—
11:00	4.68	41.26	4.08	-2.25	1.48
13:15	-0.49	-0.07	1.18	-0.18	-0.19
14:45	-2.10	-3.24	—	-2.50	—

Table S3: Diatom cells (L sediment)⁻¹ in depth sections over the course of day. The ± symbol corresponds to standard deviation. Data was used for Figure 4b. Shaded rows indicate exposure of the cores to darkness.

		diatom cells (L sediment) ⁻¹ in depth section				
		0 – 0.5 cm	0.5 – 1 cm	1 – 2 cm	2 – 3 cm	3 – 4 cm
Time of day (hh:mm)	16:00	1.91±0.2 10 ⁸	3.06 ±1.44 10 ⁷	6.37±1.80 10 ⁶	3.82 ±1.80 10 ⁶	2.55 ±3.60 10 ⁶
	18:00	1.63±0.5 10 ⁸	8.15±0.7 10 ⁷	6.37 ±9.00 10 ⁶	1.27 ±1.80 10 ⁶	6.37 ±1.80 10 ⁶
	21:00	1.78±0.2 10 ⁸	1.02 ±0.07 10 ⁸	4.71±1.26 10 ⁷	2.55 ±0.3 10 ⁷	1.27±0.3 10 ⁷
	05:00	1.78±0.2 10 ⁸	2.80±1.08 10 ⁷	5.09±3.24 10 ⁷	4.84±2.16 10 ⁷	1.66 ±0.5 10 ⁷
	11:00	1.68±0.5 10 ⁸	6.11±0 10 ⁷	2.67±1.27 10 ⁷	7.64 10 ⁶ ±6.59	6.37 ±12.7 10 ⁵
	14:00	2.24±0.5 10 ⁸	1.27±1.08 10 ⁷	6.37±1.80 10 ⁶	2.55±0 10 ⁶	1.27±1.80 10 ⁶

Supplementary References

- Eren AM, Maignien L, Sul WJ, Murphy LG, Grim SL, Morrison HG, Sogin ML (2013) Oligotyping: Differentiating between closely related microbial taxa using 16S rRNA gene data. *Methods Ecol Evol* 4 (12):1111-1119. doi:10.1111/2041-210x.12114
- Kozich JJ, Westcott SL, Baxter NT, Highlander SK, Schloss PD (2013) Development of a Dual-Index Sequencing Strategy and Curation Pipeline for Analyzing Amplicon Sequence Data on the MiSeq Illumina Sequencing Platform. *Applied and Environmental Microbiology* 79 (17):5112. doi:10.1128/AEM.01043-13
- Lange-Bertalot, H. and Metzeltin, D. (1996) Indicators of oligotrophy - 800 taxa representative of three ecologically distinct lake types, Carbonate buffered - Oligodystrophic - Weakly buffered soft water. Lange-Bertalot, H. (ed.), *Iconographia Diatomologica. Annotated Diatom Micrographs. Vol. 2. Ecology, Diversity, Taxonomy.* Koeltz Scientific Books. Königstein, Germany, 2:390 pp.
- Lange-Bertalot, H. (2001) *Navicula sensu stricto*, 10 genera separated from *Navicula sensu lato*, *Frustulia Diatoms of Europe 2: 1-526*
- Seekatz AM, Theriot CM, Molloy CT, Wozniak KL, Bergin IL, Young VB (2015) Fecal Microbiota Transplantation Eliminates *Clostridium difficile* in a Murine Model of Relapsing Disease. *Infection and Immunity* 83 (10):3838. doi:10.1128/IAI.00459-15